

Electromagnetic effects induced by time-dependent axion field

Katsuhisa Taguchi,¹ Tatsushi Imaeda,² Tetsuya Hajiri,³ Takuya Shiraiishi,⁴ Yukio Tanaka,² Naoya Kitajima,⁴ and Tatsuhiro Naka^{4,5}

¹*Yukawa Institute for Theoretical Physics, Kyoto University, Kyoto 606-8502, Japan*

²*Department of Applied Physics, Nagoya University, Nagoya 464-8603, Japan*

³*Department of Materials Physics, Nagoya University, Nagoya 464-8603, Japan*

⁴*Department of Physics, Nagoya University, Nagoya 464-8602, Japan*

⁵*Kobayashi Masukawa Institute for the Origin of Particles and the Universe, Nagoya 464-8602, Japan*

(Dated: April 7, 2024)

We studied the dynamics of the so-called θ -term, which exists in topological materials and is related to a hypothetical field predicted by Peccei-Quinn in particle physics, in a magnetic superlattice constructed using a topological insulator and two ferromagnetic insulators, where the ferromagnetic insulators had perpendicular magnetic anisotropies and different magnetic coercive fields. We examined a way to drive the dynamics of the θ -term in the magnetic superlattice through changing the inversion symmetry (from an anti-parallel to a parallel magnetic configuration) using an external magnetic field. As a result, we found that unconventional electromagnetic fields, which are magnetic field-induced charge currents and vice versa, are generated by the nonzero dynamics of the θ -term.

Introduction.— In the context of high-energy physics, an axion is an additional scalar degree of freedom, which gives a natural solution to the charge conjugation parity problem in the standard model of particle physics[1]. In the cosmological context, it can also take the role of dark matter in the present universe, and the axion detection experiment is currently one of the most exciting fields of study. The axion couples with electromagnetic fields \mathbf{E} and \mathbf{B} as follows:

$$\mathcal{L}_a = \frac{\alpha}{2\pi} g \frac{a(t)}{f_a} \mathbf{E} \cdot \mathbf{B}, \quad (1)$$

where α is a fine structure constant, g is a coefficient of $\mathcal{O}(1)$ [2–5], $a(t)$ is the (time-dependent) axion field, and f_a is the so-called Peccei-Quinn scale. Because of an extremely small value of $a(t)/f_a \lesssim 10^{-19}$ in the present universe, it is difficult to detect the signature of a dark-matter axion.

Intriguingly, a Lagrangian similar to Eq. (1) can be realized in topological materials:

$$\mathcal{L}_\theta = \frac{e^2}{2\pi h} \theta \mathbf{E} \cdot \mathbf{B}, \quad (2)$$

where e is an elementary charge, and the term proportional to θ is the so-called θ -term. This is analogous to $a(t)/f_a$ in Eq. (1), but θ is basically a static constant in the time-reversal symmetry. The finite θ can be realized in the family of topological insulators (TIs), which includes magnetic-doped TIs[6, 7], multilayers of magnetic TIs[8, 9], Weyl semimetals (WSs)[10–13], and superlattices[14–16]. In the presence of θ , characteristic electromagnetic effects, [16–23], anomalous Hall effects[24–28], chiral magnetic effects[29–37], and Kerr effects[38, 39], have been intensively studied.

One of the most interesting physical phenomena driven by the θ -term is the electromagnetic effect via the dynamics of θ (i.e., $\partial_t \theta$), which could be analogous to the axion.

So far, the unconventional optical effect [40] and electric field-induced magnetic field [41] have been discussed under a nonzero $\partial_t \theta$, whose dynamics is caused by magnetic fluctuations, in materials with breaking time-reversal and inversion symmetries. Then, the time-average of $\partial_t \theta$ becomes zero, and its manipulation by an external field might be difficult.

In this letter, we discuss a way to drive the dynamics of the θ -term using an external magnetic field and consider the electromagnetic effects via $\partial_t \theta$ in a magnetic superlattice while breaking both the time- and inversion-reversal symmetries. The magnetic superlattice we consider is constructed using a TI and two ferromagnetic insulators (FIs) [FI1/TI/FI2/spacer] $_n$ [Fig. 1(a)], where FI1 and FI2 have perpendicular magnetic anisotropies and different magnetic coercive fields. Here, to clearly define the θ -term, we consider the axion insulator phase realized in the FI/TI superlattice [Fig. 1(b)]. Then, θ can correspond to magnetic configurations of the FIs, where the inversion-reversal symmetry is preserved or broken corresponding to parallel (P) or anti-parallel (AP) magnetic configurations. These configurations could be controlled by an external magnetic field because of the different magnetic coercive fields. Through this control, the nonzero $\partial_t \theta$ is induced during the AP \rightarrow P process. Furthermore, we found unconventional electromagnetic effects under a nonzero $\partial_t \theta$. Unlike the conventional (static) electromagnetic effects, a dynamical magnetic field-induced charge current is generated and vice versa.

Model.— We start with a model in the superlattice constructed by [FI1/TI/FI2/spacer] $_n$ as shown in Fig. 1(a). Its effective Hamiltonian model can be described

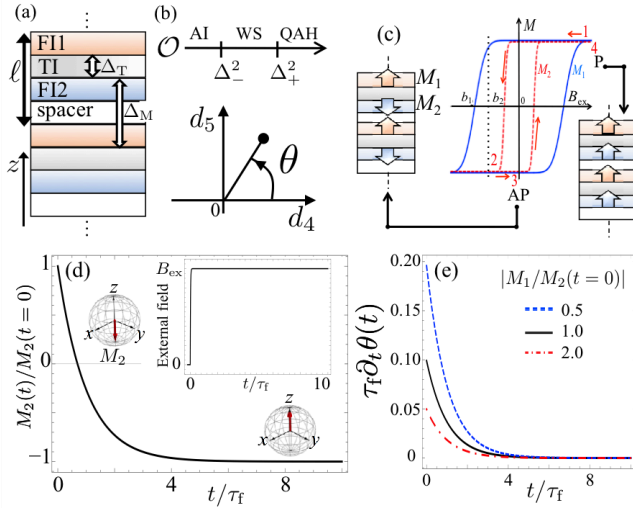


FIG. 1. (Color online) (a) Superlattice constructed by [F11/TI/F12/spacer] $_n$. (b) Phase diagram of superlattice, which is categorized by an order parameter $\mathcal{O} = M_1 M_2$ with several tunneling parameter $\Delta_{\pm} = \Delta_T \pm \Delta_M$. In the AI phase ($\mathcal{O} < \Delta_-^2$), the θ -term is given by $\theta = \tan^{-1}(d_5/d_4)$ within the lowest order of M_+ . (c) Illustration of the magnetic hysteresis loops and magnetic configurations of the superlattice with different magnetic coercive fields (b_1 and b_2) under an external magnetic field \mathbf{B}_{ex} along the layered direction. M_1 and M_2 correspond to the magnetizations of the FIs. The antiparallel (AP) and parallel (P) magnetic configurations can be generated by \mathbf{B}_{ex} though $1 \rightarrow 2 \rightarrow 3$ (red arrows) and $3 \rightarrow 4$, respectively. (d) Time-dependence of $M_2(t)$ by the external magnetic field \mathbf{B}_{ex} (inset) during the $3 \rightarrow 4$ process. (e) Time-dependence of the dynamical θ -term with several $|M_1/M_2(t=0)|$ at $M_1 = 0.01$ eV.

by [14, 42]

$$H = \sum_{n,m} \int d\mathbf{k}_{\parallel} \psi_{\mathbf{k}_{\parallel},n}^{\dagger} \mathcal{H}_{nm}(\mathbf{k}_{\parallel}) \psi_{\mathbf{k}_{\parallel},m}, \quad (3)$$

$$\mathcal{H}_{nm}(\mathbf{k}_{\parallel}) = h_0(\mathbf{k}_{\parallel})\delta_{n,m} + h_1\delta_{n,m+1} + h_2\delta_{n,m-1}, \quad (4)$$

$$h_0(\mathbf{k}_{\parallel}) = \hbar v \tau_z (\boldsymbol{\sigma} \times \mathbf{k}_{\parallel})_z + \Delta_T \tau_x s_0 + \mathcal{M}, \quad (5)$$

$$h_1 = \frac{1}{2} \Delta_M (\tau_x + i\tau_y) s_0, \quad (6)$$

$$h_2 = \frac{1}{2} \Delta_M (\tau_x - i\tau_y) s_0, \quad (7)$$

$$\mathcal{M} = -\frac{1}{2} M_1 (\tau_0 + \tau_z) s_z - \frac{1}{2} M_2 (\tau_0 - \tau_z) s_z, \quad (8)$$

where the creation operator $\psi_{\mathbf{k}_{\parallel},n}^{\dagger} = (\psi_{+, \uparrow, \mathbf{k}_{\parallel}, n}^{\dagger} \ \psi_{+, \downarrow, \mathbf{k}_{\parallel}, n}^{\dagger} \ \psi_{-, \uparrow, \mathbf{k}_{\parallel}, n}^{\dagger} \ \psi_{-, \downarrow, \mathbf{k}_{\parallel}, n}^{\dagger})$ of an electron, where \uparrow and \downarrow are the spin indices and $+$ and $-$ indicate the top and bottom of the same TI layer, respectively. The labels n and m indicate the TI layers, and $\hbar \mathbf{k}_{\parallel}$ and v are the momentum and velocity of the surface states of a TI layer, respectively. Δ_T (Δ_M) denotes the tunneling between the top and bottom of the same TI layer (of neighboring TI layers). s_0 (τ_0)

and $s_{x,y,z}$ ($\tau_{x,y,z}$) are a 2×2 identical matrix and Pauli matrices acting on the spin (the surface) degrees of freedom, respectively. \mathcal{M} indicates the exchange interaction of the FIs, where M_1 and M_2 correspond to the z -components of the magnetizations of F1 and F2, respectively. $\ell = L/N$ is the superlattice period, and L is the length of the whole layer. In the limit $N \rightarrow \infty$, the effective Hamiltonian is also described by a Fourier transformed form as follows [14, 42]:

$$H = \int d\mathbf{k} \psi_{\mathbf{k}}^{\dagger} \left[\sum_{n=1}^5 d_n(\mathbf{k}) \Gamma^n + M_+ \tau_0 s_z \right] \psi_{\mathbf{k}} \quad (9)$$

with $d_{n=1,2,3,4,5} = [-\hbar v k_x, \hbar v k_y, -\Delta_M \sin k_z \ell, \Delta_T + \Delta_M \cos k_z \ell, M_-]$, $\mathbf{k} = (k_x, k_y, k_z)$, $M_{\pm} \equiv (M_1 \pm M_2)/2$, and $\Gamma^{n=1,2,3,4,5} = (\tau_z s_y, \tau_z s_x, \tau_y s_0, \tau_x s_0, \tau_z s_z)$, which is defined by $\{\Gamma^n, \Gamma^m\} = 2\delta^{nm}$.

The dispersion of the Hamiltonian is given by $\epsilon^2(\mathbf{k}) = \hbar^2 v^2 k_{\parallel}^2 + [M_+ \pm \sqrt{M_-^2 + \Delta_{k_z}^2}]^2$ with $\Delta_{k_z}^2 = \Delta_M^2 + \Delta_T^2 + 2\Delta_M \Delta_T \cos k_z \ell$. Based on this, the gap-full state, *i.e.*, axion insulator (AI) and quantum anomalous Hall (QAH) systems are characterized by the conditions $\mathcal{O} > \Delta_-^2$ and $\mathcal{O} > \Delta_+^2$, respectively, where $\mathcal{O} \equiv M_+^2 - M_-^2 = M_1 M_2$ is an order parameter in the superlattice [Fig. 1(b)]. The gapless phase (WS phase) is realized for $\Delta_-^2 < \mathcal{O} < \Delta_+^2$.

The θ -term was studied in the AI phase and WS phase. The former is clearly described by $\delta\theta = \tan^{-1}(d_5/d_4)$ within the lowest order of M_+ [Fig. 1(b)], and the latter is given by the distance of each point-node of the dispersion [14]. In the following, to discuss the dynamical θ -term clearly, we focus on the AI phase.

Electromagnetic effect via $\delta\theta$.— The electromagnetic effects in the AI phase can be given by [17–20, 43, 44]

$$\begin{aligned} \mathcal{L} &= \mathcal{L}_{\text{Maxwell}} + \mathcal{L}_{\theta} + \mathcal{L}_e \\ &= \frac{1}{2} [\epsilon E^2 - \frac{1}{\mu} B^2] + \frac{e^2}{2\pi\hbar} (\theta_0 + \delta\theta) \mathbf{E} \cdot \mathbf{B} + \mathbf{j}_e \cdot \mathbf{A} \end{aligned} \quad (10)$$

Here, \mathcal{L}_e denotes the gauge coupling between charge current \mathbf{j}_e and vector potential \mathbf{A} . ϵ and μ are the electrical permittivity and magnetic permeability of the medium, respectively. θ_0 ($= 0$ or π) is a static value and $\delta\theta$ denotes the deviation from θ_0 [40–42, 45, 46]. Below, we simply consider $\delta\theta$ in the linear response of d_5 and $d_4 \sim \Delta_+$. Then, $\delta\theta$ is given by [34, 42]

$$\delta\theta = \tan^{-1} \left[\frac{M_-}{\Delta_+} \right]. \quad (11)$$

The Maxwell equations are given by

$$\begin{aligned} \nabla \times \mathbf{E} &= -\partial_t \mathbf{B} \\ \nabla \times \mathbf{B}/\mu &= \epsilon \partial_t \mathbf{E} + \mathbf{j}_e + \mathbf{j}_{\theta}, \end{aligned} \quad (12)$$

where $\mathbf{j}_{\theta} = -[(\nabla \delta\theta) \times \mathbf{E} + (\partial_t \delta\theta) \mathbf{B}] c \epsilon \alpha / \pi$ is a charge current due to $\delta\theta$, and c is the velocity of light. Then, the wave equation becomes

$$(\partial_t^2 - c^2 \nabla^2) \mathbf{B} = \frac{1}{\epsilon} \nabla \times (\mathbf{j}_e + \mathbf{j}_{\theta}). \quad (13)$$

The right-hand side of the above equation indicates the source term for the wave equation. The first term is conventional but the second term, which depends on $\nabla\delta\theta$ and $\partial_t\delta\theta$, is unconventional and is given by $\nabla \times \mathbf{j}_\theta/\epsilon = -\frac{c\alpha}{\pi} [(\nabla \cdot \mathbf{E})\nabla\delta\theta - (\nabla\delta\theta) \cdot \nabla\mathbf{E}] - \frac{c\alpha\mu}{\pi}\partial_t\delta\theta(\epsilon\partial_t\mathbf{E} + \mathbf{j}_e + \mathbf{j}_\theta)$. In particular, for $\nabla\delta\theta = 0$ and $\nabla \times \mathbf{j}_e = 0$, the wave equation becomes

$$(\partial_t^2 - c^2\nabla^2)\mathbf{B} = -\frac{c\alpha\mu}{\pi}\partial_t\delta\theta(\epsilon\partial_t\mathbf{E} + \mathbf{j}_e + \mathbf{j}_\theta). \quad (14)$$

Dynamics of $\delta\theta$.— To drive the nonzero dynamics of θ ($\partial_t\delta\theta$), we focus on magnetic configurations in the superlattice. Here, we assume that the magnetizations of FI1 and FI2 have perpendicular magnetic anisotropies and different magnetic coercive fields b_1 and b_2 , as illustrated in Fig. 1(c). Then, an external magnetic field $\mathbf{B}_{\text{ex}} = B_{\text{ex}}\hat{z}$ along the layered direction can trigger a change in the magnetic configurations (\hat{z} is a unit vector). For example, first we set the AP magnetic configuration, which can be generated through the $1 \rightarrow 2 \rightarrow 3$ process, with $b_1 < B_{\text{ex}} < b_2$, as shown in Fig. 1(c). Then, the AP magnetic configuration becomes stable even when $B_{\text{ex}} = 0$. After $B_{\text{ex}} \neq 0$ is applied, the M_2 values of the FIs are changed by B_{ex} , and the magnetic configuration can be dynamically changed from the AP configuration to the P magnetic configuration via the $3 \rightarrow 4$ process. The changes in the magnetic configurations are caused by the change in the magnetization of FI2, which is switched from the $-z$ to the $+z$ direction during $3 \rightarrow 4$. The above process could drive the nonzero $\partial_t\delta\theta$.

The magnetization switch can be phenomenologically understood using the Bloch equation for the magnetization motion as $\partial_t M_2(t) = [M_2(t=0) - M_2(t)]/\tau_f$, where τ_f is the characteristic relaxation time of the magnetization switching, which depends on the material. To solve this equation, we assume the initial condition $M_2(t=0) = -M_2$ with $M_2 > 0$, as illustrated in Fig. 1(d). Then, we have $M_2(t) = M_2[1 - 2\exp(-t/\tau_f)]$ for $M_-(t) = [M_1 - M_2(t)]/2$ [Fig. 1(d)]. As a result, $\partial_t\delta\theta$ is given by Eq. (11) as follows:

$$\partial_t\delta\theta(t) = \frac{\Delta_+ M_2 \exp(-t/\tau_f)}{\Delta_+^2 + M_-^2(t)} \frac{1}{\tau_f}. \quad (15)$$

Using the $\partial_t\delta\theta$ [Fig. 1(e)], we consider the following three cases. Below, we simply focus on the time-dependence of \mathbf{B} and $\partial_t\delta\theta$, and we ignore $c^2\nabla^2\mathbf{B}$ and set $\nabla\delta\theta = 0$.

$\partial_t\delta\theta$ -induced magnetic field and charge current.— We consider the responses by the dynamical θ term $\partial_t\delta\theta(t)$ during the $3 \rightarrow 4$ process under a static external magnetic field $\mathbf{B}_{\text{ex}} = B_{\text{ex}}\hat{z}$, which is applied at $t = 0$. Here, we focus on the unconventional magnetic field $[\mathbf{B}_\theta(t)]$ via a nonzero $\partial_t\delta\theta$, which can be defined and decomposed as $\mathbf{B}(t) \equiv \mathbf{B}_{\text{ex}} + \mathbf{M}_+(t) + \mathbf{B}_\theta(t)$. Then, the time-revolution of $\mathbf{B}_\theta(t)$ is given from $\partial_t^2\mathbf{B}(t) = [\frac{\alpha}{\pi}\partial_t\delta\theta]^2\mathbf{B}(t)$:

$$\partial_t^2\mathbf{B}_\theta = \frac{\alpha^2}{\pi^2}(\partial_t\delta\theta)^2(\mathbf{B}_\theta + \mathbf{B}_{\text{ex}} + \mathbf{M}_+) - \partial_t^2\mathbf{M}_+. \quad (16)$$

To solve this, we use the following final and initial conditions:

$$\begin{aligned} \mathbf{B}_\theta(t \rightarrow +\infty) &= 0 \\ \partial_t\mathbf{B}_\theta(t=0) &= -\partial_t\mathbf{M}_+(t)|_{t \rightarrow 0}, \end{aligned} \quad (17)$$

where the former indicates the removal of a divergent solution, and the latter is determined from $\partial_t\mathbf{B}(t) = -\nabla \times \mathbf{E}$ at $t = 0$, while assuming $\nabla \times \mathbf{E} \rightarrow 0$ at $t = 0$.

Figure 2 illustrates the dynamical θ -term that induces magnetic field \mathbf{B}_θ . The nonzero \mathbf{B}_θ is only generated during the $3 \rightarrow 4$ process. Furthermore, from Eq. (12), the $\partial_t\delta\theta$ couples with the external magnetic field and drives the charge current $\mathbf{j}_\theta = -[\partial_t(\delta\theta)]\mathbf{B}_{\text{ex}}c\epsilon\alpha/\pi$ only during $3 \rightarrow 4$, as described in Fig. 2. This magnetic-field induced charge current can be regarded as a kind of chiral magnetic effect[29–37].

Under charge current along \mathbf{B}_{ex} .— Next, we discuss the magnetic field via $\partial_t\delta\theta$ in the presence of both the magnetic field $\mathbf{B}_{\text{ex}} = B_{\text{ex}}\hat{z}$ and the charge current $\mathbf{j}_e = j_e\hat{z}$, which is spatially uniform. Then, the time-revolution of $\mathbf{B}_\theta = B_\theta\hat{z}$ becomes

$$\begin{aligned} \partial_t^2 B_\theta &= \frac{\alpha^2}{\pi^2}(\partial_t\delta\theta)^2(B_\theta + B_{\text{ex}} + M_+) - \partial_t^2 M_+ \\ &\quad - \frac{c\alpha\mu_0}{\pi}\partial_t\delta\theta j_e. \end{aligned} \quad (18)$$

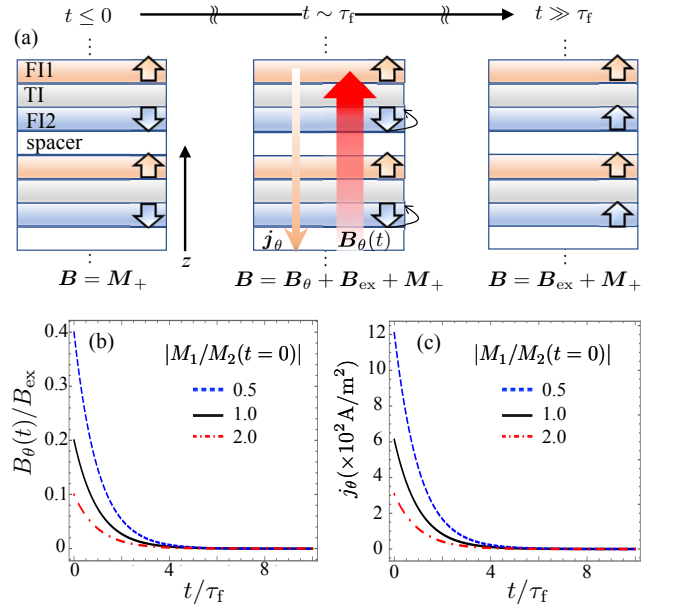


FIG. 2. (Color online) Dynamical θ term induces magnetic field \mathbf{B}_θ and charge current \mathbf{j}_θ . (a) Illustration of \mathbf{B}_θ (red arrows) and \mathbf{j}_θ (orange arrows) in the presence of the dynamical θ term during the $3(t \leq 0) \rightarrow 4(t \gg \tau_f)$ process. \mathbf{B}_{ex} is an external magnetic field and $\mathbf{M}_+ = [M_1 + M_2(t)]\hat{z}$ corresponds to the total magnetization of the FIs. (b) Time-dependence of B_θ and (c) time-dependence of j_θ . We use the parameters $\Delta_+ = 0.1$ eV, $M_1 = 10$ meV, $\tau_f = 1$ ns, $\epsilon = 8.8 \times 10^{-12}$ F/m, and $B_{\text{ex}} = 0.1$ T.

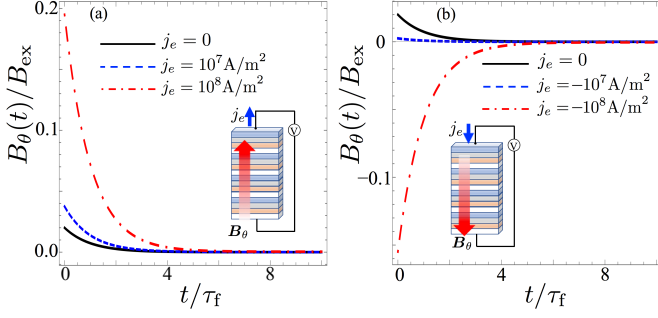


FIG. 3. (Color online) Time-dependence of magnetic field $B_\theta \equiv B_\theta(j_e = 0) + B_\theta(j_e \neq 0)$ due to $\partial_t \delta\theta$ in presence of external magnetic field \mathbf{B}_{ex} and charge current $\mathbf{j}_e = j_e \hat{z}$ along layered direction in (a) $j_e > 0$ and (b) $j_e < 0$, with several j_e at $|M_1/M_2(t=0)| = 1$. The parameters are the same as those used in Fig. 2.

$B_\theta \equiv B_\theta(j_e = 0) + B_\theta(j_e \neq 0)$ is generated not only by the coupling between $\partial_t \delta\theta$ and \mathbf{B}_{ex} but also by the coupling between $\partial_t \delta\theta$ and \mathbf{j}_e . The former $B_\theta(j_e = 0)$ is given in Fig. 2. The latter $B_\theta(j_e \neq 0)$ will be dominant when the magnitude of j_e is sufficiently large (Fig. 3). It should be noted that during the $3 \rightarrow 4$ process, the charge current via the chiral magnetic effect j_θ is also generated, and the charge current j_e includes j_θ as $j_e \rightarrow j_e + j_\theta$. However, the magnitude of j_θ is smaller than the sufficient value of current (e.g., 10^7 A/m^2) [see Fig. 2(c)]. Hence, the small j_θ hardly affects B_θ .

Charge current perpendicular to \mathbf{B}_{ex} .— We consider B_θ in the presence of the external magnetic field $\mathbf{B}_{\text{ex}} = B_{\text{ex}} \hat{z}$ and the charge current $\mathbf{j}_e = j_e \hat{z}$. Then, we have

$$\partial_t^2 B_{\theta,z} = \frac{\alpha^2}{\pi^2} (\partial_t \delta\theta)^2 (B_{\theta,z} + B_{\text{ex}} + M_+) - \partial_t^2 M_+, \quad (19)$$

$$\partial_t^2 B_{\theta,x} = -\frac{c\alpha\mu_0}{\pi} \partial_t \delta\theta j_e. \quad (20)$$

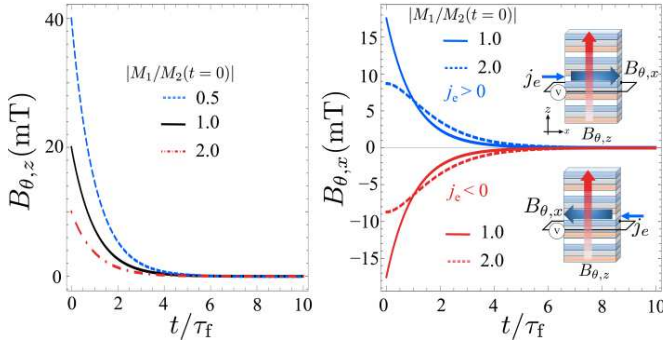


FIG. 4. (Color online) Magnetic field $\mathbf{B}_\theta = B_{\theta,z} \hat{z} + B_{\theta,x} \hat{x}$ induced by dynamics of θ under charge current along x direction ($\mathbf{j}_e = j_e \hat{x}$). (a) Time-dependence of $B_{\theta,z}$ with several $|M_1/M_2|$ [see also Fig. 2(b)]. (b) Time-dependence of $B_{\theta,x}$ at $j_e = \pm 10^7 \text{ A/m}^2$ with $|M_1/M_2(t=0)| = 1, 2$. The parameters are the same as those used in Fig. 2. (inset) Illustration of the magnetic fields due to the dynamics of θ .

The induced magnetic field $\mathbf{B}_\theta = B_{\theta,z} \hat{z} + B_{\theta,x} \hat{x}$ is solved under the initial condition [Eq. (17)], and it can be decomposed into two terms. $B_{\theta,z}$ is the same magnetic field $B_\theta(j_e = 0)$ parallel to \mathbf{B}_{ex} [Fig. 4(a)], and $B_{\theta,x}$ corresponds to the same magnetic field $B_\theta(j_e \neq 0)$ parallel to \mathbf{j}_e [Fig. 4(b)].

It should be noted that $B_{\theta,x}$ is the current-induced magnetic field. The direction of $B_{\theta,x}$ is parallel to the applied charge current direction, which is different from that of the charge currents via Ampère's law. In addition, $B_{\theta,x}$ is regarded as a kind of electromagnetic effect (current-induced magnetic field) or Edelstein effect. The conventional current-induced magnetic field [47–49] is represented by $\mathcal{B}_m = \chi_{mn} j_{e,n}$, where \mathcal{B}_m is an induced magnetic field, $j_{e,n}$ is a static charge current, and $\chi_{mn}(m, n = x, y, z)$ is a coefficient that is usually determined by the characteristic parameters in an equilibrium state in materials. Hence, χ_{mn} is static. On the other hand, $B_{\theta,x}(t)$ is described by the form $B_{\theta,x} = \chi_{\theta,xn}(t) j_{e,n}$, where the coefficient $\chi_{\theta,xn}$ is represented by

$$\chi_{\theta,xn}(t) = -\frac{c\alpha\mu_0}{\pi} \delta_{xn} \left[\int_0^t dt_1 \delta\theta(t_1) + c_1 t + c_2 \right]. \quad (21)$$

Here, c_1 and c_2 are arbitrary constants determined by the initial condition. Because the theta-term $\delta\theta$ is dynamical, $\chi_{\theta,xn}$ is dynamical, unlike the conventional χ_{mn} .

Finally, we discuss an experimental instrument for the obtained results in the response to the dynamics of θ . Although we consider the model in the superlattice [FI1/TI/FI2/spacer] $_n$ to study a simple model of $\partial_t \theta$, the number of ferromagnetic metals is practically larger than that of the FIs. Recently, for example, an axion-insulator multilayer constructed of a TI film and Cr-doped TI film with different magnetic coercive fields was experimentally studied [8]. A superlattice of tailored axion-insulators could be used for the model we considered. In such materials, it is expected that the manipulation of the magnetic configurations of FIs (AP and P) is driven by an external magnetic field along the layered direction, as illustrated in Fig. 2(a). As a result, the dynamics of θ can be driven via the AP \rightarrow P process. Then, three electromagnetic effects occur during the process. First, the chiral magnetic effect, which is a magnetic field-induced charge current, could be expected. In other words, in the absence of an applied charge current, the chiral magnetic effect, which is caused by the dynamical θ -term and applied magnetic field, drives a charge current of $\approx 10^2 \text{ A/m}^2$ [Fig. 2(c)], which could be detectable. Second, another electromagnetic effect is $B_{\theta,z}$, which is driven by the dynamics of the θ -term and the external magnetic field \mathbf{B}_{ex} . The magnitude of $B_{\theta,z}$, for example, becomes $\approx 20 \text{ mT}$ during a few tens of τ_f [Fig. 4(a)]. We expect that it could be difficult to distinguish $B_{\theta,z}$ from the total magnetic field \mathbf{B} [Fig. 2(a)] because the magnetic fields are in the same direction. Third, the obtained electromagnetic effect is the

current-induced magnetic field $B_{\theta,x}$, which occurs when we apply the charge current. Under the in-plane charge current \mathbf{j}_e , $B_{\theta,x}$, which is along the applied current direction, reaches $\approx \pm 10\text{mT}$ when $M_1 = M_2 = 10\text{ meV}$ and $d_4 = 0.1\text{ eV}$ with $j_e = \pm 10^7\text{ A/m}^2$. This current-induced magnetic field could be measurable by manipulations of the current direction. It should be noted that under the in-plane charge current, a spin-transfer-torque-induced magnetic field[50–52] could also be generated by the coupling between the applied current and magnetizations on the surfaces of the TIs. However, this magnetic field could be much smaller than that of $B_{\theta,x}$, which would make it experimentally negligible.

Conclusion.— We have theoretically studied a way to drive the dynamics of θ in a magnetic superlattice with an axion insulator phase. As a result, we have shown the unconventional electromagnetic effects via $\partial_t\theta$: The dynamical magnetic field-induced charge current, which is a kind of chiral magnetic effect, and the current-induced magnetic effect, which is a kind of Edelstein effect, have been discussed. The obtained results, including the artificial control of $\partial_t\theta$ by an external field, could be analogous to the time-dependent axion field $a(t)/f_a$ in dark-matter axion physics.

This work was supported by the institute for advanced research (IAR) in Nagoya University through a Grant-in-Aid. In addition, this work was supported by a Grant-in-Aid for Scientific Research on Innovative Areas, Topological Material Science (No. JP15H05853), and a Grant-in-Aid for Challenging Exploratory Research (Grant No. JP15K13498 and 16K13803) from the Ministry of Education, Culture, Sports, Science, and Technology, Japan (MEXT). K.T. also gives thanks for the support of the Core Research for Evolutional Science and Technology (CREST) of the Japan Science and Technology Corporation (JST) [JPMJCR14F1]. N.K. acknowledges the support by Grant-in-Aid for JSPS Fellows.

-
- [1] R. D. Peccei and H. R. Quinn, Phys. Rev. Lett. **38**, 1440 (1977).
 [2] M. Dine, W. Fischler, and M. Srednicki, Physics Letters B **104**, 199 (1981).
 [3] A. R. Zhitnitsky, Sov. J. Nucl. Phys. **31**, 260 (1980).
 [4] J. E. Kim, Phys. Rev. Lett. **43**, 103 (1979).
 [5] M. Shifman, A. Vainshtein, and V. Zakharov, Nuclear Physics B **166**, 493 (1980).
 [6] C.-Z. Chang, J. Zhang, X. Feng, J. Shen, Z. Zhang, M. Guo, K. Li, Y. Ou, P. Wei, L.-L. Wang, Z.-Q. Ji, Y. Feng, S. Ji, X. Chen, J. Jia, X. Dai, Z. Fang, S.-C. Zhang, K. He, Y. Wang, L. Lu, X.-C. Ma, and Q.-K. Xue, Science **340**, 167 (2013).
 [7] T. Hirahara, S. V. Ereemeev, T. Shirasawa, Y. Okuyama, T. Kubo, R. Nakanishi, R. Akiyama, A. Takayama, T. Hajiri, S.-i. Ideta, M. Matsunami, K. Sumida, K. Miyamoto, Y. Takagi, K. Tanaka, T. Okuda, T. Yokoyama, S.-i. Kimura, S. Hasegawa, and E. V. Chulkov, Nano Letters **0** (2017).
 [8] M. Mogi, M. Kawamura, R. Yoshimi, A. Tsukazaki, Y. Kozuka, N. Shirakawa, K. S. Takahashi, M. Kawasaki, and Y. Tokura, Nat Mater, 4855 (2017).
 [9] Q. L. He, X. Kou, A. J. Grutter, G. Yin, L. Pan, X. Che, Y. Liu, T. Nie, B. Zhang, S. M. Disseler, B. J. Kirby, W. Ratcliff II, Q. Shao, K. Murata, X. Zhu, G. Yu, Y. Fan, M. Montazeri, X. Han, J. A. Borchers, and K. L. Wang, Nat Mater **16**, 94 (2017).
 [10] S.-M. Huang, S.-Y. Xu, I. Belopolski, C.-C. Lee, G. Chang, B. Wang, N. Alidoust, G. Bian, M. Neupane, C. Zhang, S. Jia, A. Bansil, H. Lin, and M. Z. Hasan, Nat. Commun. **6**, 7373 (2015).
 [11] S.-Y. Xu, I. Belopolski, N. Alidoust, M. Neupane, G. Bian, C. Zhang, R. Sankar, G. Chang, Z. Yuan, C.-C. Lee, S.-M. Huang, H. Zheng, J. Ma, D. S. Sanchez, B. Wang, A. Bansil, F. Chou, P. P. Shibayev, H. Lin, S. Jia, and M. Z. Hasan, Science **349**, 613 (2015).
 [12] B. Q. Lv, H. M. Weng, B. B. Fu, X. P. Wang, H. Miao, J. Ma, P. Richard, X. C. Huang, L. X. Zhao, G. F. Chen, Z. Fang, X. Dai, T. Qian, and H. Ding, Phys. Rev. X **5**, 031013 (2015).
 [13] H. Weng, C. Fang, Z. Fang, B. A. Bernevig, and X. Dai, Phys. Rev. X **5**, 011029 (2015).
 [14] A. A. Burkov and L. Balents, Phys. Rev. Lett. **107**, 127205 (2011).
 [15] J. Tominaga, a. V. Kolobov, P. Fons, T. Nakano, and S. Murakami, Adv. Mater. Interfaces **1**, 1300027 (2014).
 [16] J. Tominaga, A. V. Kolobov, P. J. Fons, X. Wang, Y. Saito, T. Nakano, M. Hase, S. Murakami, J. Herfort, and Y. Takagaki, Sci. Technol. Adv. Mater. **16**, 14402 (2015).
 [17] A. M. Essin, J. E. Moore, and D. Vanderbilt, Phys. Rev. Lett. **102**, 146805 (2009).
 [18] X.-L. Qi, T. L. Hughes, and S.-C. Zhang, Phys. Rev. B **78**, 195424 (2008).
 [19] X.-L. Qi, R. Li, J. Zang, and S.-C. Zhang, Science **323**, 1184 (2009).
 [20] A. Karch, Phys. Rev. Lett. **103**, 171601 (2009).
 [21] G. Rosenberg and M. Franz, Phys. Rev. B **82**, 035105 (2010).
 [22] M. M. Vazifeh and M. Franz, Phys. Rev. B **82**, 233103 (2010).
 [23] Y. Lan, S. Wan, and S.-C. Zhang, Phys. Rev. B **83**, 205109 (2011).
 [24] R. Yu, W. Zhang, H.-J. Zhang, S.-C. Zhang, X. Dai, and Z. Fang, Science **329**, 61 (2010).
 [25] K. Nomura and N. Nagaosa, Phys. Rev. Lett. **106**, 166802 (2011).
 [26] J. Wang, B. Lian, X.-L. Qi, and S.-C. Zhang, Phys. Rev. B **92**, 081107 (2015).
 [27] A. A. Zyuzin and A. A. Burkov, Phys. Rev. B **86**, 1 (2012).
 [28] K. N. Okada, Y. Takahashi, M. Mogi, R. Yoshimi, A. Tsukazaki, K. S. Takahashi, N. Ogawa, M. Kawasaki, and Y. Tokura, Nat. Commun. **7**, 12245 (2016).
 [29] A. Vilenkin, Phys. Rev. D **22**, 3080 (1980).
 [30] D. E. Kharzeev, L. D. McLerran, and H. J. Warringa, Nuclear Physics A **803**, 227 (2008).
 [31] K. Fukushima, D. E. Kharzeev, and H. J. Warringa, Phys. Rev. D **78**, 074033 (2008).
 [32] M. M. Vazifeh and M. Franz, Phys. Rev. Lett. **111**, 027201 (2013).

- [33] H. Sumiyoshi and S. Fujimoto, Phys. Rev. Lett. **116**, 166601 (2016).
- [34] A. Sekine and K. Nomura, Phys. Rev. Lett. **116**, 96401 (2016).
- [35] K. Taguchi, T. Imaeda, M. Sato, and Y. Tanaka, Phys. Rev. B **93**, 201202 (2016).
- [36] Q. Li, D. E. Kharzeev, C. Zhang, Y. Huang, I. Pletikosić, A. V. Fedorov, R. D. Zhong, J. A. Schneeloch, G. D. Gu, T. Valla, I. Pletikosić, A. V. Fedorov, R. D. Zhong, J. A. Schneeloch, G. D. Gu, and T. Valla, Nat. Phys. **12**, 550 (2016).
- [37] T. Hayata, arXiv:1705.09926.
- [38] W.-K. Tse and A. H. MacDonald, Phys. Rev. Lett. **105**, 057401 (2010).
- [39] J. Maciejko, X.-L. Qi, H. D. Drew, and S.-C. Zhang, Phys. Rev. Lett. **105**, 166803 (2010).
- [40] R. Li, J. Wang, X.-L. Qi, and S.-C. Zhang, Nat Phys **6**, 284 (2010).
- [41] H. Ooguri and M. Oshikawa, Phys. Rev. Lett. **108**, 161803 (2012).
- [42] J. Wang, B. Lian, and S.-C. Zhang, Phys. Rev. B **93**, 45115 (2016).
- [43] P. Sikivie, Phys. Rev. Lett. **51**, 1415 (1983).
- [44] P. Sikivie, Phys. Rev. D **32**, 2988 (1985).
- [45] J. Wang, R. Li, S.-C. Zhang, and X.-L. Qi, Phys. Rev. Lett. **106**, 126403 (2011).
- [46] Y.-L. Lee, H. C. Park, J. Ihm, and Y.-W. Son, Proceedings of the National Academy of Sciences **112**, 11514 (2015).
- [47] E. Dzyaloshinskii, I, Sov. Phys. JETP **10**, 628 (1960).
- [48] D. N. Astrof, Sov. Phys. JETP **11**, 708 (1960).
- [49] M. Fiebig, Journal of Physics D: Applied Physics **38**, R123 (2005).
- [50] I. Garate and M. Franz, Phys. Rev. Lett. **104**, 146802 (2010).
- [51] T. Yokoyama, J. Zang, and N. Nagaosa, Phys. Rev. B **81**, 241410 (2010).
- [52] A. Sakai and H. Kohno, Phys. Rev. B **89**, 165307 (2014).